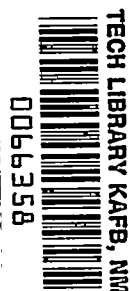NACA TN 3684

9990

NATIONAL ADVISORY COMMITTEE FOR AERONAUTICS

TECHNICAL NOTE 3684

LARGE DEFLECTION OF CURVED PLATES

By H. G. Lew, J. A. Fox, and T. T. Loo

The Pennsylvania State University

NACA

Washington

October 1956

LARGE DEFLECTION OF CURVED PLATES

By H. G. Lew, J. A. Fox, and T. T. Loo

SUMMARY

Several problems on the large deflections of curved plates with compound curvature are treated. The large-deflection equations of plates and of cylinders are used. The effect of initial curvature for a plate under axial compression is to increase its deflection considerably upon the application of load. With increasing loads, the deflection curves merge into one regardless of the initial deflection form. It is shown also that the average shear strain for a plate under shear loading is not much affected by the initial curvature, at least for the initial deflection function used. In addition, for the circular cylindrical plate with small initial curvature under axial compression, the deflections of the plate are affected more by changes in the radius R_0 than by changes in the initial curvature.

It is shown that the effective width of the curved plates in longitudinal compression is reduced by the presence of an initial deflection function.

INTRODUCTION

The present report treats several problems on the large deflection of curved plates with compound curvature which are typical of aircraft structural elements. These elements are acted upon by edge loads (axial or shear) and the stresses and deflections are investigated for loads causing deflections of the order of the thickness of the plate elements.

The work is divided into two parts. In the first part, the large deflection of a plate with small initial curvature is investigated for two loading conditions: axial (compression) and shear. In the second part, the large deflection of a curved plate element with small initial curvature from a circular cylindrical shape is considered.

In addition to the determination of the deflection and stresses the effective widths are calculated for several cases.

A right-hand xyz coordinate system is used in this report. Rectangular-plan-form plates are considered and the origin of the coordinates is taken for each problem as given in figures 1, 2, and 3.

SYMBOLS

A_q, B_q, C_r, D_r coefficients given in appendix B

a, b, l sheet dimensions

B_1 functions of w_{mn} and δ_{mn}; used in equation (12)

C coefficient used in equation (28)

C_q unknown coefficients of complementary stress function (see eq. (13))

$D = Eh^3/12(1 - \nu^2)$

d total width of sheet, any coordinate system

d_e effective width of sheet (see fig. 7(a))

E modulus of elasticity

F, F_{qr}, F_{st} any stress function and stress-function coefficients

F_c complementary solution of equation (13)

F_0 particular integral of F

G shear modulus

h thickness of shell or plate

$k = w_{0_{max}}/a^2$

k_1, k_2 constants in equation (16)

$$M_q = \cosh \frac{qb\pi}{2a} + \frac{qb\pi/2a}{\sinh \frac{qb\pi}{2a}}$$

m,n,q,r,s,t constants

max   maximum value; used as a subscript

P   surface load

P_x load per unit length of edge

$\overline{p_x},\overline{p_y}$ average compressive stresses in x- and y-directions, respectively

R_O radius of circular cylindrical curved plate from which compound curved plate is a deviation

U   strain energy of bending and stretching

u,v,w   displacements in x-, y-, and z-directions, respectively

$\bar{u}$ average displacement

u_O initial displacement

V   total potential energy

W   potential energy of applied load

w,w_{mn} total deflection and coefficient of total deflection

w_O,δ_{mn} initial deflection and coefficient of initial deflection

w_c deflection at center of plate

w_1 additional deflection

x,y,z   coordinates of a point

$\alpha = w_{O_{max}}/a$

$\epsilon_x{}',\epsilon_y{}',\gamma_{xy}{}'$ median-fiber strains

$\epsilon_x{}'',\epsilon_y{}'',\gamma_{xy}{}''$ extreme-fiber bending and shearing strains

$\overline{\epsilon_x}$ average edge strain

ν Poisson's ratio

σ_{xy} fiber stress

$\sigma_x{}',\sigma_y{}',\sigma_{xy}{}'$ median-fiber stresses

$\sigma_x{}'',\sigma_y{}'',\sigma_{xy}{}''$ extreme-fiber bending and shearing stresses

$\overline{(\ )}$ average value

LARGE DEFLECTION OF CURVED PLATES

Flat Plates With Small Initial Curvature

Equations of equilibrium.- The equations governing the large deflection of a thin curved plate in which the deflections are still small enough to use the simplified formulas for the curvatures have been derived by Von Kármán and by Marguerre (ref. 1) and can be written as

$$\nabla^4 F = E\left[\left(\frac{\partial^2 w_1}{\partial x\,\partial y}\right)^2 - \frac{\partial^2 w_1}{\partial x^2}\frac{\partial^2 w_1}{\partial y^2} + 2\frac{\partial^2 w_1}{\partial x\,\partial y}\frac{\partial^2 w_0}{\partial x\,\partial y} - \right.$$
$$\left. \frac{\partial^2 w_1}{\partial x^2}\frac{\partial^2 w_0}{\partial y^2} - \frac{\partial^2 w_0}{\partial x^2}\frac{\partial^2 w_1}{\partial y^2}\right] \tag{1}$$

and

$$\nabla^4 w = \frac{P}{D} + \frac{h}{D}\left[\frac{\partial^2 F}{\partial y^2}\frac{\partial^2(w_1 + w_0)}{\partial x^2} + \frac{\partial^2 F}{\partial x^2}\frac{\partial^2(w_1 + w_0)}{\partial y^2} - 2\frac{\partial^2 F}{\partial x\,\partial y}\frac{\partial^2(w_1 + w_0)}{\partial x\,\partial y}\right] \tag{2}$$

Equation (1) represents the compatibility equations for the median-fiber strains for a plate with an initial middle surface deflection w_0. These strains are

$$\left. \begin{aligned}
\epsilon_x{}' &= \frac{\partial u}{\partial x} + \frac{1}{2}\left(\frac{\partial w}{\partial x}\right)^2 - \frac{1}{2}\left(\frac{\partial w_0}{\partial x}\right)^2 \\[2mm]
\epsilon_y{}' &= \frac{\partial v}{\partial y} + \frac{1}{2}\left(\frac{\partial w}{\partial y}\right)^2 - \frac{1}{2}\left(\frac{\partial w_0}{\partial y}\right)^2 \\[2mm]
\gamma_{xy}{}' &= \frac{\partial u}{\partial y} + \frac{\partial v}{\partial x} + \frac{\partial w}{\partial x}\frac{\partial w}{\partial y} - \frac{\partial w_0}{\partial x}\frac{\partial w_0}{\partial y}
\end{aligned} \right\} \tag{3}$$

Equation (2) is the equilibrium equation taking into account the initial deflection w_0 of the middle surface. The additional deflection appears in the left side since it involves bending moments which depend only on the change in curvature while the slopes on the right depend on the total deflection.

In addition, the median-fiber stresses and strains are

$$
\left.
\begin{aligned}
\sigma_x' &= \frac{\partial^2 F}{\partial y^2} \\[2mm]
\sigma_y' &= \frac{\partial^2 F}{\partial x^2} \\[2mm]
\sigma_{xy}' &= -\frac{\partial^2 F}{\partial x\,\partial y} \\[2mm]
\epsilon_x' &= \frac{1}{E}\left(\frac{\partial^2 F}{\partial y^2} - \nu\,\frac{\partial^2 F}{\partial x^2}\right) \\[2mm]
\epsilon_y' &= \frac{1}{E}\left(\frac{\partial^2 F}{\partial x^2} - \nu\,\frac{\partial^2 F}{\partial y^2}\right) \\[2mm]
\gamma_{xy}' &= -2\,\frac{(1+\nu)}{E}\,\frac{\partial^2 F}{\partial x\,\partial y}
\end{aligned}
\right\}
\tag{4}
$$

The extreme-fiber bending and shearing stresses are

$$
\left.
\begin{aligned}
\sigma_x'' &= -\frac{Eh}{2(1-\nu^2)}\left(\frac{\partial^2 w_1}{\partial x^2} + \nu\,\frac{\partial^2 w_1}{\partial y^2}\right) \\[2mm]
\sigma_y'' &= -\frac{Eh}{2(1-\nu^2)}\left(\frac{\partial^2 w_1}{\partial y^2} + \nu\,\frac{\partial^2 w_1}{\partial x^2}\right) \\[2mm]
\sigma_{xy}'' &= -\frac{Eh}{2(1+\nu)}\,\frac{\partial^2 w_1}{\partial x\,\partial y}
\end{aligned}
\right\}
\tag{5}
$$

The strain energy of stretching and bending of the plate is given by

$$U = \frac{h}{2E} \iint \left\{ (\sigma_x' + \sigma_y') - 2(1 + \nu)\left[\sigma_x'\sigma_y' - (\tau_{xy}')^2\right] \right\} dx \, dy +$$

$$\frac{D}{2} \iint \left\{ (\nabla^2 w_1)^2 - 2(1 - \nu)\left[\frac{\partial^2 w_1}{\partial x^2} \frac{\partial^2 w_1}{\partial y^2} - \left(\frac{\partial^2 w_1}{\partial x \, \partial y}\right)^2\right] \right\} dx \, dy \qquad (6)$$

Note that

$$\iint \left[\frac{\partial^2 w_1}{\partial x^2} \frac{\partial^2 w_1}{\partial y^2} - \left(\frac{\partial^2 w_1}{\partial x \, \partial y}\right)^2\right] dx \, dy = 0$$

if w_1 is zero at the edges. Thus, the total potential energy is

$$V = U + W \qquad (7)$$

where W is the potential energy of the applied loads. The multiple integration is taken over the area of the plate.

Plates with normal edge loads.- The coordinate system used for and the manner of loading plates with normal edge loads are shown in figure 1.

Since this theory will be applied to plates with symmetric initial deflections and loads the assumption that there is symmetry about the center lines of the plate will be used here. The following boundary conditions appear to be reasonable representations of such plate elements:

(1) The resultant load is constant in the x-direction (zero load in y-direction); that is,

$$P_x b = h \int_0^b \sigma_x' \, dy = -\overline{p_x} hb = \text{Constant}$$

where P_x is the load per unit length of the edge.

(2) The edges $x = 0$ and $x = a$ are straight.

(3) Shearing stresses are zero at all edges.

For this case the potential energy of the applied load for normal edge loads along the edges $x = 0$ and $x = a$ is

$$W = - \oint \left(\sigma_x{}'u\right)_{x=0,a} dy \tag{8}$$

It is convenient, with the coordinate system shown in figure 1, to assume w and w_0 as a double sine series in x and y. Hence, let

$$w = \sum_{m=1,2,3,\ldots}^{\infty} \sum_{n=1,2,3,\ldots}^{\infty} w_{mn} \sin \frac{m\pi x}{a} \sin \frac{n\pi y}{b} \tag{9}$$

$$w_0 = \sum_{m=1,2,3,\ldots}^{\infty} \sum_{n=1,2,3,\ldots}^{\infty} \delta_{mn} \sin \frac{m\pi x}{a} \sin \frac{n\pi y}{b} \tag{10}$$

Upon substitution of equations (9) and (10) into equation (1), it is seen that a particular integral for F will be

$$F = - \frac{\overline{p_x}y^2}{2} + \sum_{q=0,1,2,\ldots}^{\infty} \sum_{r=0,1,2,\ldots}^{\infty} F_{qr} \cos \frac{q\pi x}{a} \cos \frac{r\pi y}{b} \tag{11}$$

where $\overline{p_x}$ is the average compressive stress in the x-direction. The value of F_{qr} in terms of the unknown coefficients w_{mn} and δ_{mn} is

$$F_{qr} = \frac{E}{4\left(q^2 \frac{b}{a} + r^2 \frac{a}{b}\right)^2} \sum_{i=1}^{\infty} B_i \tag{12}$$

Values of F_{qr} are tabulated in table 1 and the quantities B_i are functions of w_{mn} and δ_{mn}.

The requirement that only one pair of edges $x = 0$ and $x = a$ is loaded and that the other pair is stress free adds a complementary solution to F (eq. (11)). This function is

$$F_c = - \sum_{q=1,2,3,\ldots}^{\infty} C_q \cos \frac{q\pi x}{a} \left\{ \left(1 + \frac{q\pi b}{2a} \coth \frac{q\pi b}{2a}\right) \cosh \frac{q\pi}{a}\left(y - \frac{b}{2}\right) - \right.$$

$$\left. \frac{q\pi}{a}\left[y - \frac{b}{2} \sinh \frac{q\pi}{a}\left(y - \frac{b}{2}\right)\right] \right\} \tag{13}$$

Assertion of the boundary condition

$$\sigma_y' = 0 \tag{14}$$

at $y = 0,b$ leads to the value for C_q of

$$C_q = \frac{\displaystyle\sum_{q=2,4,6,\ldots}^{\infty} F_{qr}}{\cosh\dfrac{q\pi b}{2a} + \dfrac{\dfrac{q\pi b}{2a}}{\sinh\dfrac{q\pi b}{2a}}} \tag{15}$$

Thus, all the boundary conditions are satisfied by these solutions. Condition (1) is satisfied by using equations (3), (11), and (14). Condition (2) can be verified if the relation between strain and displacement u is integrated. This integration leads to

$$u_{x=a} = -u_{x=0} = \int_{a/2}^{a} \left\{ \epsilon_x' - \frac{1}{2}\left[\left(\frac{\partial w}{\partial x}\right)^2 - \left(\frac{\partial w_0}{\partial x}\right)^2\right] \right\} dx$$

$$= -\frac{a}{2E}(\overline{p_x}) - \frac{\pi^2}{16a} \sum_{m=1,3,5,\ldots}^{\infty} \sum_{n=1,3,5,\ldots}^{\infty} m^2\left(w_{mn}^2 - \delta_{mn}^2\right)$$

which is a constant. The remaining condition of zero shearing stresses is obviously satisfied.

Method of Solution.- The direct method of solution utilizing the principle of minimum potential energy will be used instead of attempting to satisfy the remaining differential equation. Thus far, the stress function F is known in terms of unknown coefficients of the additional deflection $w_1(x, y)$. By the direct method, a first variation of the total potential energy set equal to zero will yield nonlinear algebraic equations for the coefficient w_{mn} which then may be solved conveniently by successive approximation.

The formation of the total potential from equation (7) by insertion of equations (9), (10), (11), and (13) leads to integrals which are listed in appendix A.

In this procedure a system of nonlinear algebraic equations is obtained for the coefficients w_{mn} in terms of the parameter of the

load $\left(\overline{hp_x}b^2/\pi^2 D\right)$. For the numerical examples given, four unknown coefficients w_{11}, w_{13}, w_{31}, and w_{33} are used. It is convenient in the solution of these algebraic equations to assume a value for w_{11} and then to transpose all nonlinear terms to the right side. A first approximation is then obtained by neglecting all nonlinear terms on the right side and solving the remaining equations by Crout's method. A second approximation is obtained by substituting the results of the first approximation in the right side of the equations and applying Crout's method. The convergence is very rapid. An example of this is shown in table 2.

The numerical results indicate that three to four coefficients w_{mn} are sufficient to represent the complete solution for practical applications. In table 2, the center deflections w_c/h using the four coefficients w_{11}, w_{13}, w_{31}, and w_{33} are given. There is also shown in this table the coefficient w_{11}/h which is equal to w_c/h if only the w_{11} coefficient is used $\left(\text{with } w_{13}, w_{31}, \text{ and } w_{33} \text{ taken equal to zero}\right)$. Thus it is seen from table 2 that the dominant coefficient is w_{11}, and in most cases the fourth coefficient w_{33} is a very small percentage of the first. This is expected since the final deflection is assumed to be of the same form as the initial deflection. That is, the plate will bend more naturally to the given initial deflection by a compressive load for small deflections.

Numerical examples are considered for two maximum initial deflection coefficients of h and $(1/3)h$ where h is the thickness of the plate. Comparison with the result from reference 2 is good if account is taken that a maximum initial deflection coefficient of $0.1h$ was used there. The deflection curves with increasing load are shown in figure 4 together with the results from linear theory. This figure shows the coincidence of results (small and large deflections) in the linear range. Moreover, all deflection curves merge for large deflections regardless of the different initial deflection amplitudes. Of course, this is physically evident; also, the merging point appears to occur outside the range of validity of the equations used.

This method of solution (Ritz method) can be easily applied to large-deflection problems of a similar nature. Further calculation, for example, can be performed for initially curved plates with the same boundary conditions as those treated above from the integrals given in appendix A. In summary, it should be mentioned again that one differential equation (for F) and the boundary conditions are satisfied exactly and the remaining differential equation is satisfied on the average by replacing it by the assertion of the minimum of the potential energy.

Plates under edge shear loads.- In this example, a square plate
with a small initial warp is considered. The plate is loaded in pure
shear along the edges which are simply supported. The coordinate system
is shown in figure 2. The warping is again treated as the initial
deflection w_0 of a flat plate. Thus, with a linear variation along
the lines of constant x or y, the initial deflection is

$$w_0 = k_1 x + k_2 y + kxy \tag{16}$$

It is apparent from equation (1) that the linear x and y terms of
the initial deflection equation (16) cannot have any influence on the
stress function F; furthermore, these linear terms do not enter strain-
energy expression (6) which is the same for this example. Thus, the
coefficient k of the xy term in expression (16) is given by

$$w_0 = kxy = \frac{w_{0_{max}}}{a^2} xy = \frac{\alpha}{a} xy \tag{17}$$

where $\alpha = w_{0_{max}}/a$; $w_{0_{max}}$ is as indicated in figure 2.

In addition to simply supported edges, the plate elements will
satisfy the following boundary conditions which appear reasonable for
physical applications. At $x = 0,a$, $\overline{\sigma_x'} = 0$ and $\overline{\sigma_{xy}'} = \overline{\sigma_{xy}}$, and,

at $y = 0,a$, $\overline{\sigma_y'} = 0$ and $\overline{\sigma_{xy}'} = \overline{\sigma_{xy}}$. It is noted that these condi-
tions are satisfied, on the average.

The deflections w_1 under load are assumed as

$$w_1 = \sum_{mn=1,2,3,\ldots}^{\infty} W_{mn} \sin \frac{m\pi x}{a} \sin \frac{n\pi y}{a} \tag{18}$$

From symmetry considerations, $W_{mn} = W_{nm}$ for all values of n and m,
and, if $m + n$ is an odd number, the terms must vanish for the same
reason. In the example chosen, the series is truncated at $n = m = 3$
since the leading terms dominate. The deflection $w = w_1 + w_0$ is then
given by the expression

$$\frac{w}{h} = 2\left[\frac{W_{11}}{h} \sin \frac{\pi x}{a} \sin \frac{\pi y}{b} + \frac{W_{13}}{h}\left(\sin \frac{\pi x}{a} \sin \frac{3\pi y}{a} + \sin \frac{3\pi x}{a} \sin \frac{\pi y}{a} \right) + \right.$$

$$\left. \frac{W_{22}}{h} \sin \frac{2\pi x}{a} \sin \frac{2\pi y}{b} + \frac{W_{33}}{h} \sin \frac{3\pi x}{a} \sin \frac{3\pi y}{b} + \ldots \right] +$$

$$\alpha\left(\frac{a}{h}\right)\left(\frac{xy}{a^2}\right) \tag{19}$$

The substitution of this expression into equation (1) yields a solution for the stress function F in the form

$$F = \frac{E}{2} \sum_{q=0}^{\infty} \sum_{r=0}^{\infty} F_{qr} \cos 2 \frac{q\pi x}{a} \cos 2 \frac{r\pi y}{b} \qquad (20)$$

The values of F_{qr} are given in table 3.

If equations (19) and (20) are substituted into strain energy expression (6), the strain energy U may be expressed in terms of the unknown parameters w_{11}, w_{13}, w_{22}, and w_{33}. The potential energy W of the applied shearing forces along the edges is

$$W = -\overline{\sigma_{xy}}h \iint \left(\frac{\partial u}{\partial y} + \frac{\partial v}{\partial x} \right) dx\, dy$$

$$= -\overline{\sigma_{xy}}ha^2 \overline{\left(\frac{\partial u}{\partial y} + \frac{\partial v}{\partial x} \right)} \qquad (21)$$

where the integration is performed over the plan form of the plate. The expression for $\overline{\left(\frac{\partial u}{\partial y} + \frac{\partial v}{\partial x} \right)}$ can be found from equation (3).

The total potential energy V (eq. (7)) is now made stationary with respect to each of the unknown parameters. The solution of the four non-linear algebraic equations follows the iterative procedure of reference 3. The results are given in table 4 and figure 5.

The problem has been evaluated numerically for $w_{O_{max}} = 0$ and $w_{O_{max}} = 8h$. The relationship between $\left(\frac{\overline{\sigma_{xy}}}{G} \right)\left(\frac{a}{h} \right)^2$ and $\overline{\left(\frac{\partial u}{\partial y} + \frac{\partial v}{\partial x} \right)}\left(\frac{a}{h} \right)^2$ in each case has been plotted in figure 5. It is noted that, in the first case of an initially flat plate, the postbuckling strength of the plate increases continuously after the critical buckling load is reached, whereas the classical small-deflection theory predicts a constant strength (broken line in fig. 5).

The stress field developed in the plate as the buckling proceeds may be readily computed from the values of the parameters w_{11}, w_{13}, w_{22}, and w_{33} by using equations (4) and (5).

In figure 5, the results of an approximate solution (ref. 3) of Von Kármán's large-deflection plate equations are plotted. This solution

assumes the form of w_1 identical with equation (19), except for a constant factor. However, somewhat more rigid edge conditions were imposed on the plate (i.e., $\epsilon_x' = 0$ at $y = 0, a$ and $\epsilon_y' = 0$ at $x = 0, a$). This accounts for the slightly larger value of $\overline{\sigma_{xy}}$ for a given value of average shear strain. It is noted that this difference is small so that it appears that the edge conditions have a small effect on the relation between applied average shear stress and average shear strain.

Nearly Cylindrically Curved Plates

The small-deflection equations of a curved plate formed from a body of revolution under edge and surface loads have been considered from the equations of equilibrium of a body of revolution in reference 4. In this section, the large deflection of curved plates with small compound curvature is investigated by modifying the large-deflection equations of a circular cylinder to include a small initial curvature. The coordinate system and an indication of the plate shape are given in figure 3.

The following equations govern the deflection of a curved plate which differs slightly from a circular cylindrical shape. It is noted that these equations immediately reduce to those of reference 5 (where other references are given) for the case of w_0 equal to zero.

The median-fiber strains are

$$
\left.
\begin{aligned}
\epsilon_x' &= \frac{\partial u}{\partial x} + \frac{1}{2}\left(\frac{\partial w_1}{\partial x}\right)^2 + \frac{\partial w_1}{\partial x}\frac{\partial w_0}{\partial x} \\[2ex]
\epsilon_y' &= \frac{\partial v}{\partial y} + \frac{1}{2}\left(\frac{\partial w_1}{\partial y}\right)^2 - \frac{w_1}{R_0} \\[2ex]
\gamma_{xy}' &= \frac{\partial u}{\partial y} + \frac{\partial v}{\partial x} + \frac{\partial w_1}{\partial x}\frac{\partial w_1}{\partial y} + \frac{\partial w_0}{\partial x}\frac{\partial w_1}{\partial y}
\end{aligned}
\right\} \tag{22}
$$

The median-fiber stresses are given by

$$
\left.
\begin{aligned}
\sigma_x' &= \frac{E}{1 - \nu^2}\left\{\frac{\partial u}{\partial x} + \frac{1}{2}\left(\frac{\partial w_1}{\partial x}\right)^2 + \frac{\partial w_1}{\partial x}\frac{\partial w_0}{\partial x} + \nu\left[\frac{\partial v}{\partial y} + \frac{1}{2}\left(\frac{\partial w_1}{\partial y}\right)^2 - \frac{w_1}{R_0}\right]\right\} \\[2ex]
\sigma_y' &= \frac{E}{1 - \nu^2}\left\{\frac{\partial v}{\partial y} + \frac{1}{2}\left(\frac{\partial w_1}{\partial y}\right)^2 - \frac{w_1}{R_0} + \nu\left[\frac{\partial u}{\partial x} + \frac{1}{2}\left(\frac{\partial w_1}{\partial x}\right)^2 + \frac{\partial w_1}{\partial x}\frac{\partial w_0}{\partial x}\right]\right\} \\[2ex]
\sigma_{xy}' &= \frac{E}{2(1 + \nu)}\left(\frac{\partial u}{\partial y} + \frac{\partial v}{\partial x} + \frac{\partial w_1}{\partial x}\frac{\partial w_1}{\partial y} + \frac{\partial w_0}{\partial x}\frac{\partial w_1}{\partial y}\right)
\end{aligned}
\right\} \tag{23}
$$

In addition to the above stress and strain expressions the equilibrium equations in the x- and y-directions are, as before,

$$\frac{\partial \sigma_x{}'}{\partial x} + \frac{\partial \sigma_{xy}{}'}{\partial y} = 0 \tag{24}$$

$$\frac{\partial \sigma_{xy}{}'}{\partial x} + \frac{\partial \sigma_y{}'}{\partial y} = 0 \tag{25}$$

If one introduces a stress function F defined by the set of expressions

$$\left. \begin{aligned} \sigma_x{}' &= \frac{\partial^2 F}{\partial y^2} \\[2mm] \sigma_y{}' &= \frac{\partial^2 F}{\partial x^2} \\[2mm] \sigma_{xy}{}' &= -\frac{\partial^2 F}{\partial x\, \partial y} \end{aligned} \right\} \tag{26}$$

and combines these with equations (22) through (24) a compatibility equation determined as

$$\nabla^4 F = E\left[\left(\frac{\partial^2 w}{\partial x\, \partial y}\right)^2 - \frac{\partial^2 w}{\partial x^2}\frac{\partial^2 w}{\partial y^2} - \frac{1}{R_o}\frac{\partial^2 w}{\partial x^2} - \frac{\partial^2 w_o}{\partial x^2}\frac{\partial^2 w}{\partial y^2}\right] \tag{27}$$

results.

In place of a third equilibrium equation relating to the sum of the forces in the normal direction to the surface, the potential energy of the system is used for the direct method of solution as in the previous cases. One notes that a first variation of the total potential will lead to the equilibrium equation normal to the surface. The median-fiber stresses and strains and the extreme-fiber bending and shearing stresses are the same as those given by equations (4) and (5) if it is remembered that the coordinates x and y here are the cylindrical-surface coordinates.

The strain-energy expression involving the sheet bending and stretching is given by equation (6). However, the boundary conditions imposed on this problem necessitate another stress function. The potential energy of the edge load will be the same as in the previous section,

namely, the average edge load times the displacement. Since the edge displacement is a constant, this amounts to expression (8) with the boundaries $x = \pm l$ substituted for $x = 0, a$. The initial deflection from the circular cylindrical shape will be taken as

$$w_o = Cx^2 \tag{28}$$

indicating a deviation of the meridian curve from straightness.

Clamped conditions with regard to the slopes at the bulkhead or stringer junctures are assumed. The reason for this assumption was that it was felt that many times the bulkheads or ribs are fairly stiff in torsion about their flanges and that the flanges are quite wide, thus presenting a nearly clamped condition to the sheet ends. Furthermore, since the plate is initially bulged along its axis, it would probably continue to bulge under load which would mean that the sheet would act as a clamped sheet across stringers as well. Obviously, other cases could be considered where nearly simple support conditions might exist. From the nature of the problem just described, it is necessary that the edges associated with the stringers move in radial lines; that is, the displacement v at the edges $y = \pm b$ must be zero. Also, it is assumed that the edges represented by bulkheads or ribs remain straight; that is, the displacements u at $x = \pm l$ are constant.

To satisfy the clamped condition the additional deflection function was assumed as the series

$$w_1 = \sum_{m=1}^{\infty} \sum_{n=1}^{\infty} \frac{w_{mn}}{4}\left(1 + \cos\frac{m\pi x}{l}\right)\left(1 + \cos\frac{n\pi y}{b}\right) \tag{29}$$

Substitution of equation (29) into equation (27) will yield an expression for a particular integral for F. It will be

$$F_o = -\frac{\overline{p_x}y^2}{2} - \frac{\overline{p_y}x^2}{2} + E\sum_{s=0}^{\infty}\sum_{t=0}^{\infty} F_{st}\cos\frac{s\pi x}{l}\cos\frac{t\pi y}{b} \tag{30}$$

where $\overline{p_x}$ and $\overline{p_y}$ are the magnitudes of the average compressive stresses in the x- and y-directions, respectively. The values of F_{st} are given in table 5 and are similar in makeup to the other problems.

Assertion of these boundary conditions adds a complementary solution to F which has the form

$$F = E \sum_{q=1}^{\infty} \cos \frac{q\pi x}{l} \left(A_q \cosh \frac{q\pi y}{l} + \frac{q\pi y}{l} B_q \sinh \frac{q\pi y}{l} \right) +$$

$$E \sum_{r=1}^{\infty} \cos \frac{r\pi y}{b} \left(C_r \cosh \frac{r\pi x}{b} + \frac{r\pi x}{b} D_r \sinh \frac{r\pi x}{b} \right) \qquad (31)$$

The values of A_q, B_q, C_r, and D_r are given in appendix B. After applying boundary conditions to the complementary solution for the purpose of determining the unknown coefficients, the displacement u is

$$u_{\pm l} = \mp \frac{l}{4} \sum_{m=1}^{\infty} \sum_{n=1}^{\infty} \sum_{r=1}^{\infty} \frac{w_{mn}w_{mr}}{16} \frac{m^2 \pi^2}{l^2} \mp \left(\frac{\overline{p_x} - \nu\overline{p_y}}{E} \right) l \pm \sum_{m=1}^{\infty} \sum_{n=1}^{\infty} C w_{mn} \frac{l}{8}$$

$$(32)$$

The expressions for the nonzero integrals of the total strain energy in terms of the undetermined deflection coefficients are given in appendix C. Again, a solution was obtained by collecting linear terms and first omitting all nonlinear terms except one which was specified. The equations were solved by Crout's method and the solutions obtained were used to evaluate the nonlinear terms which were omitted. This iterative process was carried out three or four times to yield three-place accuracy. It was most advantageous to specify w_{31} rather than w_{11} in this example for rapid convergence.

Three numerical examples were chosen for this section. One plate has radius R_0 equal to one-half the value of the other two; another has a maximum initial deflection of one-half the value of the other two and the same radius R_0 as the first case. The results indicate that the effect of initial curvature is very small on the additional deflection as compared with the effect of changing the radius R_0. The maximum additional deflections are tabulated in table 6 and the stresses are given in table 7. The maximum additional deflections for one, two, and four terms are given in table 8.

A plot of the additional deflection at the center is shown in figure 6 for the three cases considered and demonstrates graphically the effect of cylinder radius and initial curvature.

The ratio of effective width to initial width defined as the ratio of the load carried by the plate to the load the plate would have carried if the stress had been uniform and equal to Young's modulus times the average edge strain (ref. 6) is shown in figure 7. An equivalent

definition of the effective width in many cases is the ratio of the
average stress across the loaded edges to the maximum stress at the edges.
The results obtained using this definition are also shown in figure 7(a)
and clearly indicate the difference of the two definitions in the cases
considered here. The reason for this difference is the assumption of
straight edges with zero displacement of the y edges generating an
average load $\overline{p_y}$.

The effect of an initial deflection function for the curved plates
loaded in longitudinal compression is a reduction in the effective width.
In fact, the sheet deflects immediately upon loading since there is no
critical buckling load. As the load increases, the outward (negative
Z) bulging of the nearly straight circular cylinder indicates a higher
value of effective width than that obtained with the clamped flat plate
of reference 7; this is probably due to the large curvature of the basic
cylinder as compared with that of a flat plate. This is shown in fig-
ure 7(a). Figure 7(b) compares the effective width of a single finite-
length wave deflection of the problem considered here with the simply
supported very long circular cylinder of reference 6. The increase in
effective width here is due to the clamped boundary and the outward
bulging assumed. It is noted from the figures also that the change of
effective width with increasing edge strain is small.

CONCLUDING REMARKS

The problem of the large deflection of plates with compound curvature
has been considered in this report. The large-deflection plate theory
and circular-cylinder theory with an initial nonzero deflection function
are used. Three cases have been worked out completely. These are an
initially curved plate subjected to a longitudinal compressive load and
to a shear load and a curved plate, with an initial deflection from a
circular cylindrical shape, loaded with longitudinal compressive loads.

The solution by the Ritz method indicates that a very small number
of unknown coefficients (two to four, say) was sufficient to give reason-
able results even with large deflections. Thus, the stress conditions
and large deflections of curved plates (compound curvature) may be easily
obtained by such methods. Some results are shown in the figures and
tables.

The effect of an initial deflection function for the curved plates
loaded in longitudinal compression is a reduction in the effective width.
The effective width of the curved plate with almost circular cylindrical
shape is higher than that of the initially flat plate and that given by
Levy (ref. 6) for circular cylindrical curved panels.

The Pennsylvania State University,
    University Park, Pa., April 29, 1955.

APPENDIX A

INTEGRALS OF RECTANGULAR PLATE LOADED IN EDGE COMPRESSION

The deflections of a rectangular plate loaded in edge compression are given by the following expressions:

$$w = \sum_{m=1}^{\infty} \sum_{n=1}^{\infty} w_{mn} \sin \frac{m\pi x}{a} \sin \frac{n\pi y}{b}$$

$$w_O = \sum_{m=1}^{\infty} \sum_{n=1}^{\infty} \delta_{mn} \sin \frac{m\pi x}{a} \sin \frac{n\pi y}{b}$$

If Poisson's ratio is taken as 0.3 for the material together with the deflections given above, the nonzero integrals are:

$$\frac{h}{2E} \int_0^b \int_0^a \left(\sigma_x' + \sigma_y' \right)^2 dx\, dy = \frac{h}{2E} \sum_{q=2,4,6}^{\infty} \sum_{r=2,4,6}^{\infty} \frac{r^4 \pi^4 a}{4b^3} \left(1 + \frac{q^2 b^2}{r^2 a^2} \right) F_{qr}^2 -$$

$$\frac{h}{2E} \sum_{q=2,4,6}^{\infty} \sum_{r=2,4,6}^{\infty} \sum_{t=0,2,4,6}^{\infty} \frac{q^3 \pi^3}{a^2} \frac{\sinh \frac{q\pi b}{2a}}{M_p} F_{qr} F_{qt} +$$

$$\frac{h}{2E} \left(\sum_{r=2,4,6}^{\infty} \frac{r^4 \pi^4}{b^4} \frac{ab}{2} F_{0r}^2 + \sum_{q=2,4,6}^{\infty} \frac{q^4 \pi^4}{b^4} \frac{ab}{2} F_{q0}^2 \right) -$$

$$\frac{h}{E} \sum_{q=2,4,6}^{\infty} \sum_{r=0,2,4,6}^{\infty} \frac{q^3 \pi^3}{a^2} \frac{\sinh \frac{q\pi b}{2a}}{M_q} F_{qr} F_{q0} +$$

$$\frac{2h}{E} \sum_{q=2,4,6}^{\infty} \sum_{r=0,2,4,6}^{\infty} \sum_{t=0,2,4,6}^{\infty} \frac{q^3 \pi^3}{4a^2} \frac{\frac{b}{a} + \sinh \frac{q\pi b}{a}}{M_q^2} F_{qr} F_{qt} + \frac{h}{2E} \bar{p}_x^2 ab$$

$$\frac{h}{2E} \int_0^b \int_0^a -2(1 + \nu) \left[\sigma_x' \sigma_y' - (\tau')^2 \right] dx \, dy =$$

$$\frac{h}{2E} \left(2.6 \sum_{q=2,4,6}^{\infty} \sum_{r=0,2,4,6}^{\infty} \sum_{t=0,2,4,6}^{\infty} \frac{q^4 \pi^4}{4a^2} \frac{b}{a} \frac{1 - \dfrac{q^2 \pi^2}{2} \dfrac{b^2}{a^2} \coth^2 \dfrac{q\pi b}{2a}}{M_q^2} F_{qr} F_{qt} \right)$$

$$\frac{D}{2} \int_0^b \int_0^a \left[\nabla^2 (w - w_0) \right]^2 dx \, dy = \frac{abD}{8} \sum_{m=1,3}^{\infty} \sum_{n=1,3}^{\infty} \frac{\pi^4}{a^4} \left(m^2 + n^2 \frac{a^2}{b^2} \right)^2 \left(W_{mn} - \delta_{mn} \right)^2$$

$$\oint h\sigma_n' u_n \, dt = - \frac{h}{E} \overline{p_x}^2 ab - \frac{h\overline{p_x}}{8} \pi^2 \frac{b}{a} \sum_{m=1,3}^{\infty} \sum_{n=1,3}^{\infty} m^2 \left(W_{mn}^2 - \delta_{mn}^2 \right)$$

where

$$M_q = \cosh \frac{q\pi b}{2a} + \frac{\dfrac{q\pi b}{2a}}{\sinh \dfrac{q\pi b}{2a}}$$

APPENDIX B

EXPRESSIONS FOR A_q, B_q, C_r, AND D_r FOR CURVED SHEET

HAVING $1/R_0$ MUCH GREATER THAN MERIDIAN CURVATURE

When $1/R_0$ is much greater than the meridian curvature and with $\sigma_{xy}' = 0$ along all of the edges,

$$A_q = -B_q\left(1 + \frac{q\pi b}{l}\coth\frac{q\pi b}{l}\right)$$

$$C_r = -D_r\left(1 + \frac{r\pi l}{b}\coth\frac{r\pi l}{b}\right)$$

Substituting these values of A_q and C_r and assuming constant u displacement and zero v displacement will give the following values of B_q and D_r:

q	B_q
1	$\dfrac{1}{64}\dfrac{l}{b}\dfrac{\pi}{\sinh(\pi b/l)}\left(w_{11}^2 + w_{11}w_{31} + 9w_{13}^2 + 9w_{13}w_{33}\right) - \dfrac{bl}{8\pi R_0}\dfrac{\left(w_{11} + w_{13}\right)}{\sinh(\pi b/l)}$
2	$\dfrac{1}{512}\dfrac{l}{b}\dfrac{\pi}{\sinh(2\pi b/l)}\left(w_{11}^2 + 9w_{13}^2 + 2w_{11}w_{31} + 18w_{13}w_{33}\right)$
3	$\dfrac{1}{192}\dfrac{l}{b}\dfrac{\pi}{\sinh(3\pi b/l)}\left(w_{11}w_{31} + 9w_{13}w_{33} + w_{31}^2 + 9w_{33}^2\right) - \dfrac{bl}{24R_0\pi}\dfrac{\left(w_{31} + w_{33}\right)}{\sinh(3\pi b/l)}$
4	$\dfrac{1}{512}\dfrac{l}{b}\dfrac{\pi}{\sinh(4\pi b/l)}\left(w_{11}w_{31} + 9w_{13}w_{33}\right)$
6	$\dfrac{1}{1{,}536}\dfrac{l}{b}\dfrac{\pi}{\sinh(6\pi b/l)}\left(w_{31}^2 + 9w_{33}^2\right)$

r	D_r
1	$\dfrac{1}{64}\dfrac{b}{l}\dfrac{\pi}{\sinh(\pi l/b)}\left(w_{11}^2 + w_{11}w_{13} + 9w_{31}^2 + 9w_{31}w_{33}\right) - \dfrac{clb}{16\pi}\dfrac{\left(w_{11} + w_{31}\right)}{\sinh(\pi l/b)}$
2	$\dfrac{1}{512}\dfrac{b}{l}\dfrac{\pi}{\sinh(2\pi l/b)}\left(w_{11}^2 + 2w_{11}w_{13} + 9w_{31}^2 + 18w_{31}w_{33}\right)$
3	$\dfrac{1}{192}\dfrac{b}{l}\dfrac{\pi}{\sinh(3\pi l/b)}\left(w_{11}w_{13} + w_{13}^2 + 9w_{31}w_{33} + 9w_{33}^2\right) - \dfrac{clb}{48\pi}\dfrac{\left(w_{13} + w_{33}\right)}{\sinh(3\pi l/b)}$
4	$\dfrac{1}{512}\dfrac{b}{l}\dfrac{\pi}{\sinh(4\pi l/b)}\left(w_{11}w_{13} + 9w_{31}w_{33}\right)$
6	$\dfrac{1}{1{,}536}\dfrac{b}{l}\dfrac{\pi}{\sinh(6\pi l/b)}\left(w_{13}^2 + 9w_{33}^2\right)$

APPENDIX C

INTEGRALS OF RECTANGULAR DOUBLY CURVED PLATE WITH $1/R_0$

MUCH LESS THAN MERIDIAN CURVATURE

The deflections of the rectangular doubly curved plate with $1/R_0$ much less than meridian curvature are defined by the following expressions:

$$w_1 = \sum_{m=1,3,5,\ldots}^{\infty} \sum_{n=1,3,5,\ldots}^{\infty} \frac{w_{mn}}{4}\left(1 + \cos\frac{m\pi x}{l}\right)\left(1 + \cos\frac{n\pi y}{b}\right)$$

$$w_0 = Cx^2$$

With these deflections, the nonzero integrals are

$$\frac{h}{2E}\int_{-l}^{l}\int_{-b}^{b}(\sigma_x' + \sigma_y')^2\,dx\,dy = \frac{\pi^4 hE}{2lb}\sum_{s=0,1,2,\ldots}^{\infty}\sum_{t=0,1,2,\ldots}^{\infty} F_{st}^2\left(t^2\frac{l}{b} + s^2\frac{b}{l}\right)^2 +$$

$$\frac{2hlb}{E}\left(\overline{p_x}^2 + 2\overline{p_x}\overline{p_y} + \overline{p_y}^2\right) - 4E\pi^4 h\sum_{q=1,2,3,\ldots}^{\infty}\sum_{t=0,1,2,\ldots}^{\infty} F_{qt}\frac{bl\lambda_{qt}}{t\pi}\left(\frac{t^2 q^2}{l^2 b^2} + \frac{q^4}{l^4}\right)B_q(-1)^t\sinh\frac{q\pi b}{l} -$$

$$4E\pi^4 h\sum_{s=0,1,2,\ldots}^{\infty}\sum_{r=1,2,3,\ldots}^{\infty} F_{sr}\frac{bl\lambda_{sr}}{s\pi}\left(\frac{r^4}{b^4} + \frac{s^2 r^2}{l^2 b^2}\right)D_r(-1)^s\sinh\frac{r\pi l}{b} +$$

$$2E\pi^4 h\sum_{q=1,2,3,\ldots}^{\infty} B_q^2\frac{q^4}{l^2}\left(\frac{1}{2q\pi}\sinh^2\frac{q\pi b}{l} + \frac{b}{l}\right) +$$

$$4E\pi^4 h\sum_{q=1,2,3,\ldots}^{\infty}\sum_{r=1,2,3,\ldots}^{\infty} B_q D_r\frac{q^2 r^2}{l^2 b^2}\left[\frac{2b\lambda_{qr}}{r\pi}(-1)^r\sinh\frac{q\pi b}{l}\right]\left[\frac{2l\lambda_{qr}}{q\pi}(-1)^q\sinh\frac{r\pi l}{b}\right] +$$

$$2E\pi^4 h\sum_{r=1,2,3,\ldots}^{\infty} D_r^2\frac{r^4}{b^2}\left(\frac{1}{2r\pi}\sinh\frac{2r\pi l}{b} + \frac{l}{b}\right)$$

$$- \frac{h}{2E} \int_{-l}^{l} \int_{-b}^{b} 2(1 + \nu) \left[\sigma_x' \sigma_y' - \left(\sigma_{xy}' \right)^2 \right] dx \ dy = - \frac{4h}{E}(1 + \nu) l b \overline{p_x} \overline{p_y}$$

where

$$\lambda_{qr} = \frac{qr \, lb}{q^2 b^2 + r^2 l^2}$$

$$\frac{D}{2} \int_{-l}^{l} \int_{-b}^{b} \left(\nabla^2 w_1 \right)^2 = \frac{D}{2} \left\{ \frac{\pi^4 lb}{16} \left[w_{11}^2 \left(\frac{1}{l^2} + \frac{1}{b^2} \right)^2 + w_{13}^2 \left(\frac{1}{l^2} + \frac{9}{b^2} \right)^2 + \right. \right.$$

$$\left. w_{31}^2 \left(\frac{9}{l^2} + \frac{1}{b^2} \right)^2 + w_{33}^2 \left(\frac{9}{l^2} + \frac{9}{b^2} \right)^2 \right] +$$

$$\frac{\pi^4 b}{8l^3} \left(w_{11}^2 + 2w_{11}w_{13} + 81w_{31}^2 + w_{13}^2 + 162w_{31}w_{33} + 81w_{33}^2 \right) +$$

$$\frac{\pi^4 l}{8b^3} \left(w_{11}^2 + 2w_{11}w_{31} + 81w_{13}^2 + 162w_{13}w_{33} + w_{31}^2 + 81w_{33}^2 \right) \right\}$$

REFERENCES

1. Marguerre, K.: Zur Theorie der gekrümmten Platte grosser Formänderung.
   Proc. Fifth Int. Cong. Appl. Mech. (Sept. 1938, Cambridge, Mass),
   John Wiley & Sons, Inc., 1939, pp. 93-101.

2. Coan, J. M.: Large-Deflection Theory for Plates With Small Initial
   Curvature Loaded in Edge Compression. Jour. Appl. Mech., vol. 18,
   no. 2, June 1951, pp. 143-151.

3. Levy, Samuel, Fienup, Kenneth L., and Woolley, Ruth M.: Analysis of
   Square Shear Web Above Buckling Load. NACA TN 962, 1945.

4. Lew, H. G.: Bending of Thin Plates With Compound Curvature. NACA
   TN 2782, 1952.

5. Kempner, Joseph: Postbuckling Behavior of Axially Compressed Circular
   Cylindrical Shells. Jour. Aero. Sci., vol. 21, no. 5, May 1954,
   pp. 329-335.

6. Levy, Samuel: Large-Deflection Theory of Curved Sheet. NACA TN 895,
   1943.

7. Levy, Samuel, and Krupen, Philip: Large-Deflection Theory for End
   Compression of Long Rectangular Plates Rigidly Clamped Along Two
   Edges. NACA TN 884, 1943.

TABLE 1

VALUES OF F_{qr} FOR $w = \sum\limits_{m=1,3,5,\ldots}^{\infty} \sum\limits_{n=1,3,5,\ldots}^{\infty} w_{mn} \sin \frac{m\pi x}{a} \sin \frac{n\pi y}{b}$,

$w_0 = \delta_{11} \sin \frac{\pi x}{a} \sin \frac{\pi y}{b}$, AND $a/b = 1$

q	r	F_{qr}
0	2	$(E/32)\left(w_{11}^2 - \delta_{11}^2 - 2w_{11}w_{13} + 9w_{31}^2 - 18w_{31}w_{33}\right)$
0	4	$(E/64)\left(w_{11}w_{13} + 9w_{31}w_{33}\right)$
0	6	$(E/288)\left(w_{13}^2 + 9w_{33}^2\right)$
2	0	$(E/32)\left(w_{11}^2 - \delta_{11}^2 - 2w_{11}w_{31} + 9w_{13}^2 - 18w_{13}w_{33}\right)$
2	2	$(E/16)\left(w_{11}w_{31} + w_{11}w_{13} - 4w_{13}w_{31}\right)$
2	4	$(E/400)\left(-w_{11}w_{13} + 9w_{11}w_{33} + 25w_{13}w_{31}\right)$
2	6	$(E/400)\left(9w_{13}w_{33}\right)$
4	0	$(E/64)\left(w_{11}w_{31} + 9w_{13}w_{33}\right)$
4	2	$(E/400)\left(-w_{11}w_{31} + 9w_{11}w_{33} + 25w_{13}w_{31}\right)$
4	4	$(E/64)\left(-w_{13}w_{31}\right)$
4	6	$(E/2,704)\left(-9w_{13}w_{33}\right)$
6	0	$(E/288)\left(w_{31}^2 + 9w_{33}^2\right)$
6	2	$(E/400)\left(9w_{31}w_{33}\right)$
6	4	$(E/2,704)\left(-9w_{31}w_{33}\right)$

TABLE 2

NUMERICAL RESULTS FOR INITIALLY CURVED PLATE UNDER EDGE

COMPRESSION FOR VARIOUS INITIAL DEFLECTIONS

(a) $w_O = 0.333h$

w_{11}/h	$\overline{P}_x b^2 h / \pi^2 D$	w_c/h
0.35	0.176	0.351
.40	.726	.401
.50	1.503	.495
.75	2.780	.748
1.25	4.693	1.231
2.00	8.342	2.261

(b) $w_O = h$

w_{11}/h	$\overline{P}_x b^2 h / \pi^2 D$	w_c/h
1.05	0.288	1.076
1.15	.902	1.175
1.25	1.480	1.273
1.50	2.877	1.504
1.75	4.254	1.749
2.00	5.644	1.977
2.50	8.640	2.411

TABLE 3

VALUES OF F_{qr} FOR SQUARE, INITIALLY CURVED PLATE UNDER SHEAR LOADING

$$\left[F = E \sum_{q,r=0}^{6} F_{qr} \cos \frac{\pi(qx - ry)}{a} - \overline{\sigma_{xy}}xy; \quad K = \frac{2\alpha}{\pi^2} \frac{a}{h}; \right]$$

q	r	$\frac{q}{a}$	$\frac{r}{a}$	F_{qr}
2	0	0	2	$(1/8)\left(w_{11}^2 - 2w_{11}w_{13} - 18w_{13}w_{33} + 9w_{13}^2\right)$
4	0	0	4	$(1/16)\left(w_{11}w_{13} + 9w_{13}w_{33} + 2w_{22}^2\right)$
6	0	0	6	$(1/72)\left(w_{13}^2 + 9w_{33}^2\right)$
2	2	2	-2	$(1/4)\left(w_{11}w_{13} - 2w_{13}^2\right) + (1/16)w_{22}K$
2	4	2	-4	$(1/200)\left(9w_{11}w_{33} - w_{11}w_{13} + 25w_{13}^2\right)$
2	6	2	-6	$(1/200)\left(9w_{13}w_{33}\right)$
4	2	4	-2	$(1/200)\left(9w_{11}w_{33} - w_{11}w_{13} + 25w_{13}^2\right)$
6	2	6	-2	$(1/200)\left(9w_{13}w_{33}\right)$
4	6	4	-6	$(1/1,352)\left(-9w_{13}w_{33}\right)$
6	4	6	-4	$(1/1,352)\left(-9w_{13}w_{33}\right)$
4	4	4	-4	$(1/32)\left(-w_{13}^2\right)$
1	1	1	-1	$(4)\left(-w_{13}w_{22}\right) + (1/4)w_{11}K$
1	3	1	-3	$(1/50)\left(4w_{11}w_{22} + 16w_{13}w_{22}\right) + (3/100)w_{13}K$
1	5	1	-5	$(1/338)\left(16w_{13}w_{22} + 36w_{22}w_{33}\right)$
3	1	3	-1	$(1/50)\left(4w_{11}w_{22} + 16w_{13}w_{22}\right) + (3/100)Kw_{13}$
5	1	5	-1	$(1/338)\left(16w_{13}w_{22} + 36w_{22}w_{33}\right)$
3	5	3	-5	$(1/578)\left(-4w_{13}w_{22}\right)$
5	3	5	-3	$(1/578)\left(-4w_{13}w_{22}\right)$
3	3	3	-3	$(1/36)w_{33}K$

[a] Alternate values.

TABLE 4

NUMERICAL RESULTS FOR INITIALLY CURVED SQUARE PLATE UNDER SHEAR

LOADING FOR DIFFERENT INITIAL DEFLECTIONS

(a) $w_o = 0$

w_{22}/h	$\left(\overline{\dfrac{\partial u}{\partial y} + \dfrac{\partial v}{\partial x}}\right)\left(\dfrac{a}{h}\right)^2$	$\dfrac{\overline{\sigma_{xy}}a^2}{Eh^2}$	$\dfrac{\overline{\sigma_{xy}}a^2}{Gh^2}$	w_{1c}/h
0	22.087	8.495	22.087	0
.05	22.857	8.747	22.743	.392
.10	24.612	9.330	24.257	.739
.15	26.985	10.091	26.236	1.037
.20	29.698	10.939	28.441	1.295
.25	32.659	11.842	30.789	1.526
.30	35.854	12.795	33.268	1.737
.40	42.921	14.839	38.582	2.123
.50	51.005	17.100	44.461	2.479
.70	70.692	22.405	58.255	3.157
1.00	110.470	32.770	85.202	4.159

(b) $w_o = 8h$

w_{22}/h	$\left(\overline{\dfrac{\partial u}{\partial y} + \dfrac{\partial v}{\partial x}}\right)\left(\dfrac{a}{h}\right)^2$	$\dfrac{\overline{\sigma_{xy}}a^2}{Eh^2}$	$\dfrac{\overline{\sigma_{xy}}a^2}{Gh^2}$	w_{1c}/h
0.05	14.349	4.401	11.443	1.003
.10	21.897	6.647	17.282	1.438
.15	28.324	8.505	22.114	1.777
.30	47.583	13.966	36.311	2.615
.50	70.873	20.168	52.438	3.393

TABLE 5

EXPRESSIONS FOR F_{st} IN DOUBLY CURVED SHEET UNDER AXIAL COMPRESSION

$$\left[1/R_0 \text{ is much greater than meridian curvature}\right]$$

s	t	F_{st}
1	0	$\left[1\middle/\left(\frac{b}{l}\right)^2\right]\left[-\frac{w_{11}^2}{32}-\frac{w_{11}w_{31}}{32}-\frac{9w_{13}^2}{32}-\frac{9w_{13}w_{33}}{32}+\frac{b^2}{4R_0\pi^2}(w_{11}+w_{13})\right]$
2	0	$\left[1\middle/\left(\frac{4b}{l}\right)^2\right]\left(-\frac{w_{11}w_{31}}{16}-\frac{9w_{13}w_{33}}{16}-\frac{w_{11}^2}{32}-\frac{9}{32}w_{13}^2\right)$
3	0	$\left[1\middle/\left(\frac{9b}{l}\right)^2\right]\left[-\frac{9}{32}w_{11}w_{31}-\frac{9w_{31}^2}{32}-\frac{81}{32}w_{33}w_{13}-\frac{81}{32}w_{33}^2+\frac{9b^2}{4R_0\pi^2}(w_{31}+w_{33})\right]$
4	0	$\left[1\middle/\left(\frac{16b}{l}\right)^2\right]\left(-\frac{w_{11}w_{31}}{4}-\frac{9}{4}w_{13}w_{33}\right)$
6	0	$\left[1\middle/\left(\frac{36b}{l}\right)^2\right]\left(-\frac{9}{32}w_{31}^2-\frac{81}{32}w_{33}^2\right)$
0	1	$\left[1\middle/\left(\frac{l}{b}\right)^2\right]\left[-\frac{w_{11}^2}{32}-\frac{w_{11}w_{13}}{32}-\frac{9w_{31}^2}{32}-\frac{9w_{31}w_{33}}{32}+\frac{l^2c}{2\pi^2}(w_{11}+w_{31})\right]$
0	2	$\left[1\middle/\left(\frac{4l}{b}\right)^2\right]\left(-\frac{w_{11}^2}{32}-\frac{1}{16}w_{11}w_{13}-\frac{9}{32}w_{31}^2-\frac{9}{16}w_{31}w_{33}\right)$
0	3	$\left[1\middle/\left(\frac{9l}{b}\right)^2\right]\left[-\frac{9w_{11}w_{13}}{32}-\frac{9w_{13}^2}{32}-\frac{81w_{31}w_{33}}{32}-\frac{81w_{33}^2}{32}+\frac{9l^2c}{2\pi^2}(w_{13}+w_{33})\right]$
0	4	$\left[1\middle/\left(\frac{16l}{b}\right)^2\right]\left(-\frac{w_{11}w_{13}}{4}-\frac{9w_{31}w_{33}}{4}\right)$
0	6	$\left[1\middle/\left(\frac{36l}{b}\right)^2\right]\left(-\frac{9}{32}w_{13}^2-\frac{81}{32}w_{33}^2\right)$
1	1	$\left[1\middle/\left(\frac{b}{l}+\frac{l}{b}\right)^2\right]\left[-\frac{w_{11}^2}{16}-\frac{w_{11}w_{13}}{16}-\frac{w_{11}w_{31}}{16}-\frac{w_{13}w_{31}}{16}+\left(\frac{l^2c}{2\pi^2}+\frac{b^2}{4R_0\pi^2}\right)w_{11}\right]$
1	2	$\left[1\middle/\left(\frac{b}{l}+\frac{4l}{b}\right)^2\right]\left(-\frac{w_{11}^2}{32}-\frac{5w_{11}}{16}w_{13}-\frac{9}{32}w_{11}w_{33}-\frac{w_{11}w_{31}}{32}-\frac{w_{13}w_{31}}{32}\right)$
1	3	$\left[1\middle/\left(\frac{b}{l}+\frac{9l}{b}\right)^2\right]\left[-\frac{9}{16}w_{11}w_{13}-\frac{9}{16}w_{11}w_{33}-\frac{9}{16}w_{13}^2-\frac{9}{16}w_{13}w_{33}+\left(\frac{9l^2c}{2\pi^2}+\frac{b^2}{4R_0\pi^2}\right)w_{13}\right]$
1	4	$\left[1\middle/\left(\frac{b}{l}+\frac{16l}{b}\right)^2\right]\left(-\frac{5}{16}w_{11}w_{13}-\frac{9}{32}w_{11}w_{33}-\frac{w_{13}w_{31}}{32}\right)$
1	6	$\left[1\middle/\left(\frac{b}{l}+\frac{36l}{b}\right)^2\right]\left(-\frac{9}{32}w_{13}^2-\frac{9}{32}w_{13}w_{33}\right)$
2	1	$\left[1\middle/\left(\frac{4b}{l}+\frac{l}{b}\right)^2\right]\left(-\frac{w_{11}^2}{32}-\frac{w_{11}w_{13}}{32}-\frac{5}{16}w_{11}w_{31}-\frac{9}{32}w_{11}w_{33}-\frac{w_{13}w_{31}}{32}\right)$
2	2	$\left[1\middle/\left(\frac{4b}{l}+\frac{4l}{b}\right)^2\right]\left(-\frac{w_{11}w_{13}}{4}-\frac{w_{11}w_{31}}{4}-w_{13}w_{31}\right)$
2	3	$\left[1\middle/\left(\frac{4b}{l}+\frac{9l}{b}\right)^2\right]\left(-\frac{9}{32}w_{11}w_{13}-\frac{9}{32}w_{11}w_{33}-\frac{9}{32}w_{13}^2-\frac{45}{16}w_{13}w_{33}-\frac{81}{32}w_{13}w_{31}\right)$

TABLE 5.- Concluded

EXPRESSIONS FOR F_{st} IN DOUBLY CURVED SHEET UNDER AXIAL COMPRESSION

$\left[1/R_0 \text{ is much greater than meridian curvature}\right]$

s	t	F_{st}
2	4	$\left[1/\left(\frac{4b}{l} + \frac{16l}{b}\right)^2\right]\left(-\frac{9}{16}w_{11}w_{33} - \frac{25}{16}w_{13}w_{31} - \frac{w_{11}w_{13}}{16}\right)$
2	6	$\left[1/\left(\frac{4b}{l} + \frac{36l}{b}\right)^2\right]\left(-\frac{9}{4}w_{13}w_{33}\right)$
3	1	$\left[1/\left(\frac{9b}{l} + \frac{l}{b}\right)^2\right]\left[-\frac{9}{16}w_{11}w_{31} - \frac{9}{16}w_{11}w_{33} - \frac{9}{16}w_{31}^2 - \frac{9}{16}w_{31}w_{33} + \left(\frac{l^2c}{2\pi^2} + \frac{9b^2}{4R_0\pi^2}\right)w_{31}\right]$
3	2	$\left[1/\left(\frac{9b}{l} + \frac{4l}{b}\right)^2\right]\left(-\frac{9}{32}w_{11}w_{31} - \frac{9}{32}w_{31}^2 - \frac{81}{32}w_{13}w_{31} - \frac{81}{32}w_{31}w_{33} - \frac{9}{32}w_{11}w_{33} - \frac{9}{32}w_{31}w_{33}\right)$
3	3	$\left[1/\left(\frac{9b}{l} + \frac{9l}{b}\right)^2\right]\left[-\frac{81}{16}w_{13}w_{31} - \frac{81}{16}w_{13}w_{33} - \frac{81}{16}w_{31}w_{33} - \frac{81}{16}w_{33}^2 + \left(\frac{9l^2c}{2\pi^2} + \frac{9b^2}{4R_0\pi^2}\right)w_{33}\right]$
3	4	$\left[1/\left(\frac{9b}{l} + \frac{16l}{b}\right)^2\right]\left(-\frac{81}{32}w_{13}w_{31} - \frac{90}{32}w_{31}w_{33} - \frac{9}{32}w_{11}w_{33}\right)$
3	6	$\left[1/\left(\frac{9b}{l} + \frac{36l}{b}\right)^2\right]\left(-\frac{81}{32}w_{13}w_{33} - \frac{81}{32}w_{33}^2\right)$
4	1	$\left[1/\left(\frac{16b}{l} + \frac{l}{b}\right)^2\right]\left(-\frac{5}{16}w_{11}w_{31} - \frac{9}{32}w_{11}w_{33} - \frac{1}{32}w_{13}w_{31}\right)$
4	2	$\left[1/\left(\frac{16b}{l} + \frac{4l}{b}\right)^2\right]\left(-\frac{9}{16}w_{11}w_{33} - \frac{25}{16}w_{13}w_{31} - \frac{1}{16}w_{11}w_{31}\right)$
4	3	$\left[1/\left(\frac{16b}{l} + \frac{9l}{b}\right)^2\right]\left(-\frac{9}{32}w_{11}w_{33} - \frac{81}{32}w_{13}w_{31} - \frac{45}{16}w_{13}w_{33}\right)$
4	4	$\left[1/\left(\frac{16b}{l} + \frac{16l}{b}\right)^2\right]\left(-w_{13}w_{31}\right)$
4	6	$\left[1/\left(\frac{16b}{l} + \frac{36l}{b}\right)^2\right]\left(-\frac{9}{16}w_{13}w_{33}\right)$
6	1	$\left[1/\left(\frac{36b}{l} + \frac{l}{b}\right)^2\right]\left(-\frac{9}{32}w_{31}^2 - \frac{9}{32}w_{31}w_{33}\right)$
6	2	$\left[1/\left(\frac{36b}{l} + \frac{4l}{b}\right)^2\right]\left(-\frac{9}{4}w_{31}w_{33}\right)$
6	3	$\left[1/\left(\frac{36b}{l} + \frac{9l}{b}\right)^2\right]\left(-\frac{81}{32}w_{31}w_{33} - \frac{81}{32}w_{33}^2\right)$
6	4	$\left[1/\left(\frac{36b}{l} + \frac{16l}{b}\right)^2\right]\left(-\frac{9}{16}w_{31}w_{33}\right)$
6	6	$\left[1/\left(\frac{36b}{l} + \frac{36l}{b}\right)^2\right](0)$

TABLE 6

DEFLECTIONS FOR NORMAL LOADING ON CURVED PLATE WHERE $l/b = 2$

AND $1/R_0$ IS MUCH GREATER THAN MERIDIAN CURVATURE

(a) $R_0 = 0.4b^2/\pi h$

w_{31}/h	$w_0 = h$		$w_0 = h/2$	
	$\overline{p_x}b^2/E\pi^2h^2$	w_{1c}/h	$\overline{p_x}b^2/E\pi^2h^2$	w_{1c}/h
-0.25	0.689	-0.138	------	------
-.50	1.244	-.251	1.247	-0.247
-.75	1.734	-.346	------	------
-1.00	2.252	-.438	2.242	-.431
-1.25	2.858	-.531	------	------
-1.50	3.584	-.636	3.566	-.616

(b) $R_0 = 0.2b^2/\pi h$; $w_0 = h$

w_{31}/h	$\overline{p_x}b^2/E\pi^2h^2$	w_{1c}/h
-0.1	0.553	-0.058
-.2	1.061	-.112
-.3	1.529	-.163
-.4	1.971	-.210
-.5	2.392	-.256
-.6	2.802	-.300

TABLE 7

NUMERICAL VALUES OF STRESSES CALCULATED FOR DOUBLY CURVED SHEET WITH $l/b = 2$,

$1/R_0$ MUCH GREATER THAN MERIDIAN CURVATURE, AND $w_0 = h$

R_0	$\dfrac{\overline{p_x}b^2}{E\tau^2 h^2}$	x position													
		0		±l		0		0		±l		0		±l	
		y position													
		0		0		±b		0		0		±b		±b	
		$\dfrac{\sigma_x''b^2}{E\tau^2 h^2}$	$\dfrac{\sigma_y''b^2}{E\tau^2 h^2}$	$\dfrac{\sigma_x''b^2}{E\tau^2 h^2}$	$\dfrac{\sigma_y''b^2}{E\tau^2 h^2}$	$\dfrac{\sigma_x''b^2}{E\tau^2 h^2}$	$\dfrac{\sigma_y''b^2}{E\tau^2 h^2}$	$\dfrac{\sigma_x'b^2}{E\tau^2 h^2}$	$\dfrac{\sigma_y'b^2}{E\tau^2 h^2}$	$\dfrac{\sigma_x'b^2}{E\tau^2 h^2}$	$\dfrac{\sigma_y'b^2}{E\tau^2 h^2}$	$\dfrac{\sigma_x'b^2}{E\tau^2 h^2}$	$\dfrac{\sigma_y'b^2}{E\tau^2 h^2}$	$\dfrac{\sigma_x'b^2}{E\tau^2 h^2}$	$\dfrac{\sigma_y'b^2}{E\tau^2 h^2}$
$\dfrac{0.2b^2}{\pi h}$	0.553	-0.092	-0.088	0.072	0.023	0.020	0.065	-0.549	0.098	-0.542	-0.250	+0.445	1.148	-0.670	-0.309
	1.061	-.189	-.190	.144	.045	.046	.145	-1.049	.198	-1.072	-.514	-.843	.301	-1.277	-.583
	1.529	-.283	-.284	.215	.068	.068	.216	-1.504	.301	-1.469	-.762	-1.198	.457	-1.886	-.881
	1.971	-.377	-.379	.286	.091	.091	.288	-1.928	.406	-1.833	-.808	-1.524	.617	-2.453	-1.152
	2.392	-.473	-.473	.359	.114	.114	.359	-2.329	.513	-2.239	-1.001	-1.827	.783	-3.006	-1.417
	2.802	-.570	-.568	.434	.137	.136	.431	-2.714	.623	-2.583	-1.139	-2.114	.954	-3.554	-1.684
$\dfrac{0.4b^2}{\pi h}$	0.689	-0.226	-0.210	0.177	0.056	0.049	0.154	-0.667	0.140	-0.645	-0.282	-0.552	0.185	-0.850	-0.403
	1.244	-.481	-.466	.370	.117	.110	.349	-1.179	.276	-1.077	-.452	-.940	.422	-1.600	-.762
	1.734	-.717	-.669	.561	.177	.155	.492	-1.613	.424	-1.362	-.501	-1.254	.674	-2.311	-1.102
	2.252	-.961	-.852	.768	.243	.193	.609	-2.038	.530	-1.511	-.417	-1.588	.927	-3.115	-1.509
	2.858	-1.212	-.988	.999	.316	.213	.673	-2.547	.810	-1.530	-.213	-1.983	1.173	-4.090	-1.966
	3.584	-1.470	-1.186	1.217	.385	.253	.802	-3.140	.961	-1.581	.075	-2.560	1.633	-3.214	-2.546

TABLE 8

CONVERGENCE OF ADDITIONAL CENTER DEFLECTION FOR DOUBLY CURVED

SHEET UNDER NORMAL EDGE LOADS WITH $1/R_O$ MUCH

GREATER THAN MERIDIAN CURVATURE

(a) $w_O = h$; $R_O = 0.4b^2/\pi h$

$\dfrac{\bar{p}_x b^2}{E\pi^2 h^2}$	One term	Two terms	Four terms (a)
1.194	-0.177	-0.239	-0.238
2.077	-.296	-.400	-.407
3.074	-.420	-.552	-.562

(b) $w_O = h$; $R_O = 0.2b^2/\pi h$

$\dfrac{\bar{p}_x b^2}{E\pi^2 h^2}$	One term	Two terms	Four terms (a)
1.053	-0.083	-0.111	-0.111
1.932	-.150	-.205	-.205
2.709	-.208	-.288	-.288

[a]Interpolated from four-term numerical calculations

for same values of $\dfrac{\bar{p}_x b^2}{E\pi^2 h^2}$.
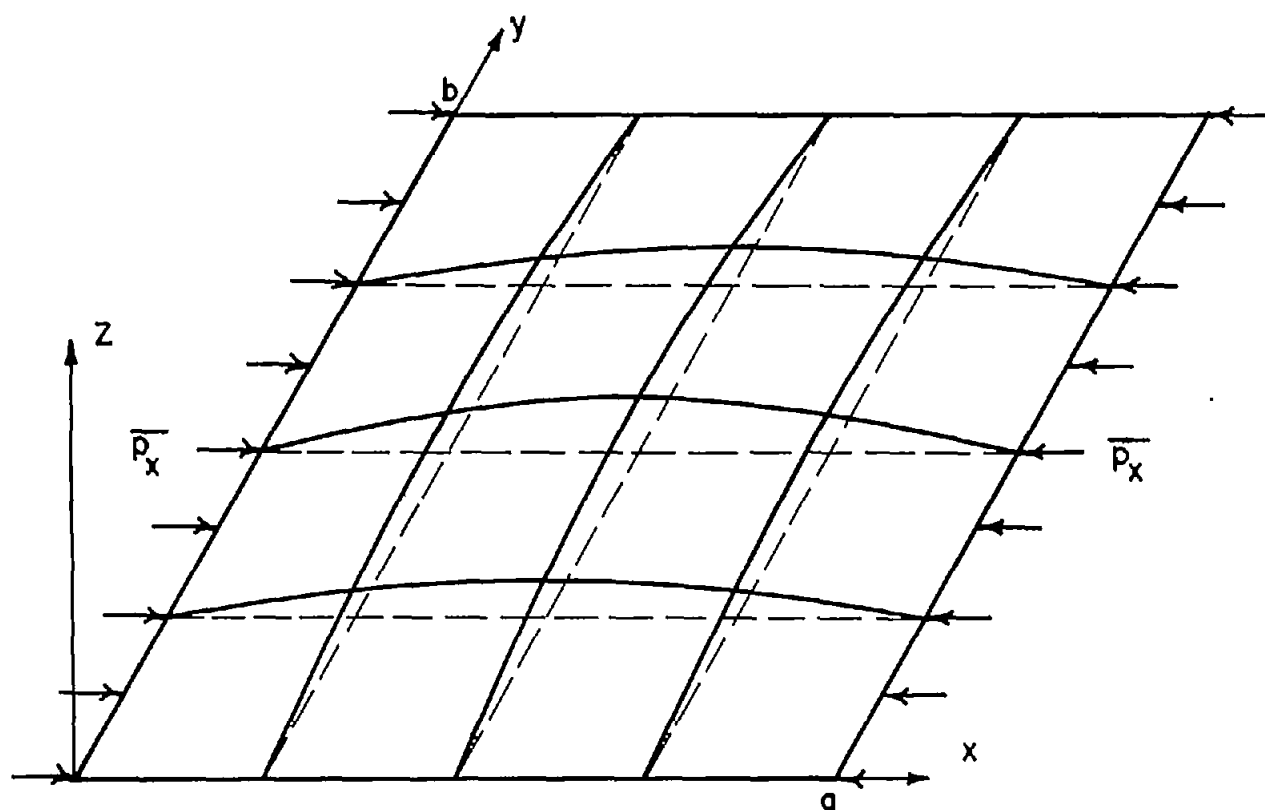
Figure 1.- Coordinate system for plates with normal edge loads.
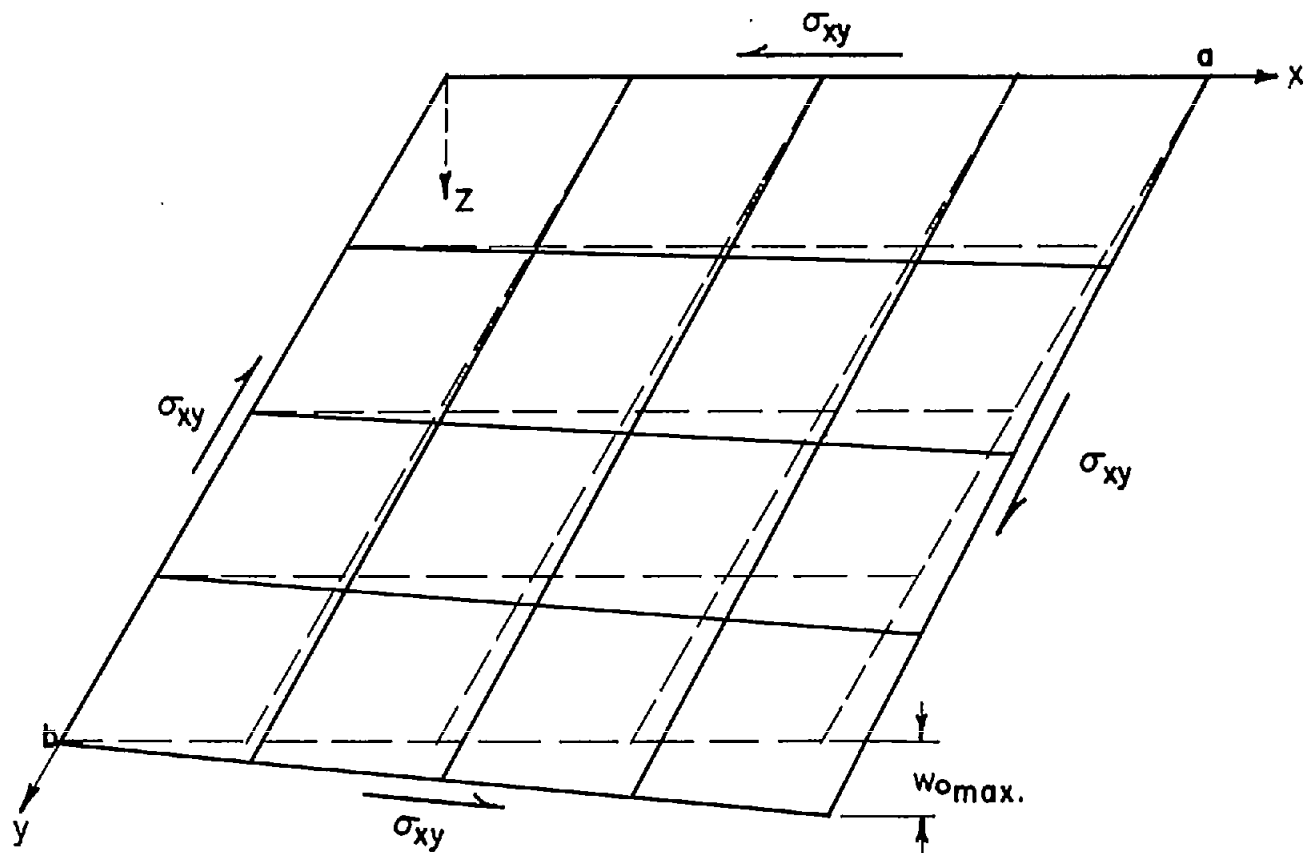
Figure 2.- Coordinate system for plates under shear loads.
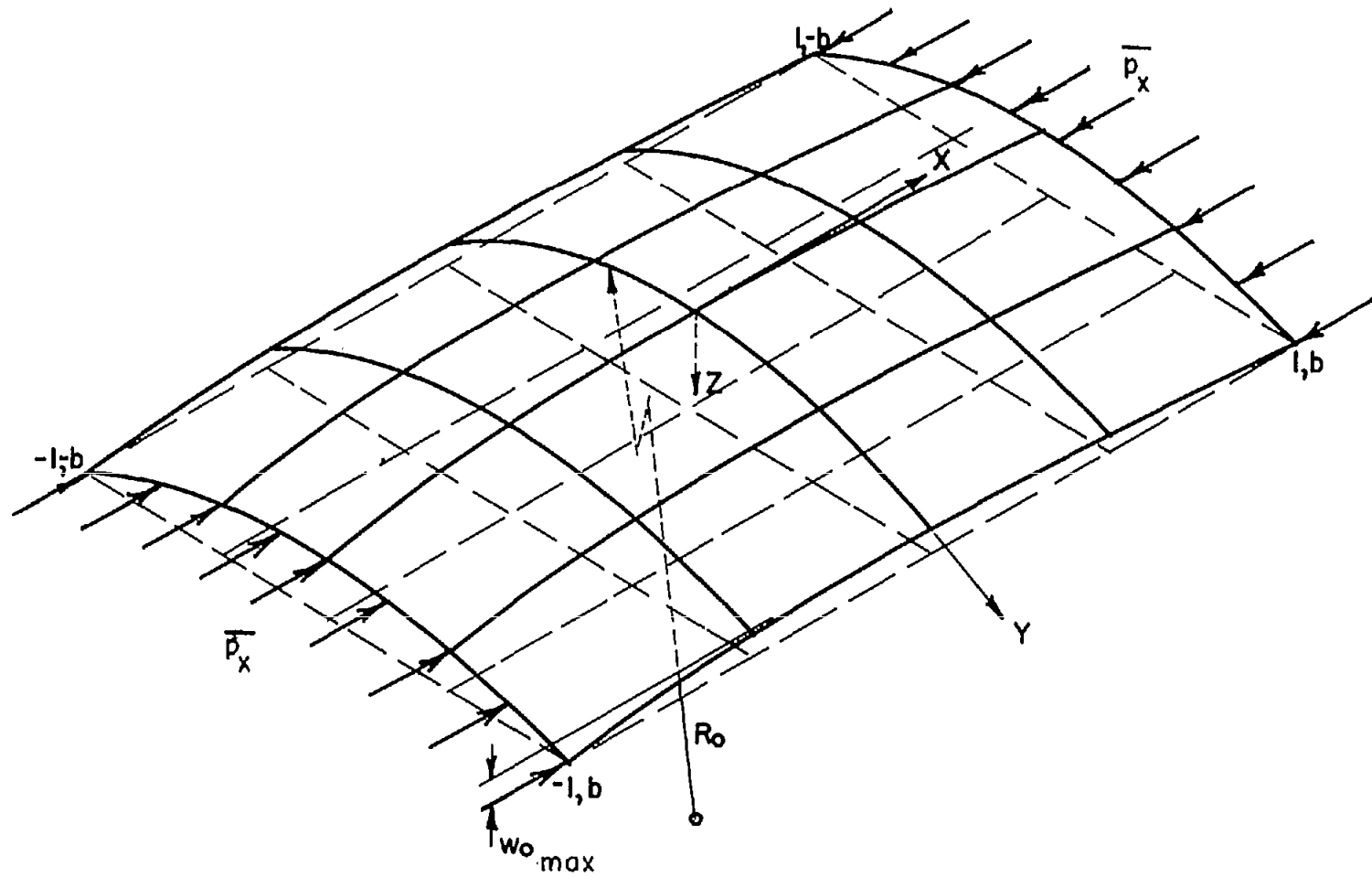
Figure 3.- Coordinate system for doubly curved sheets with $1/R_0$ much greater than meridian curvature.
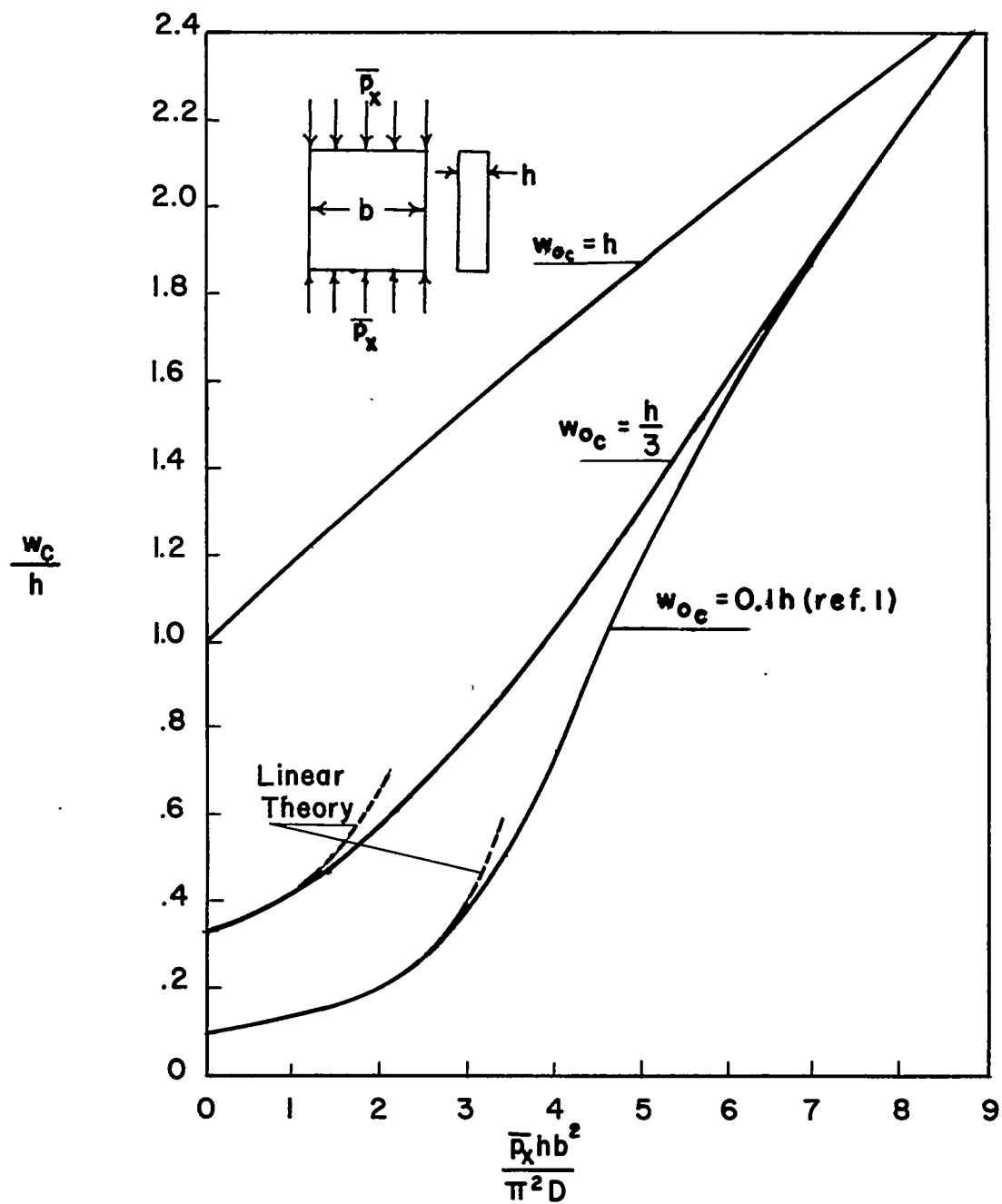
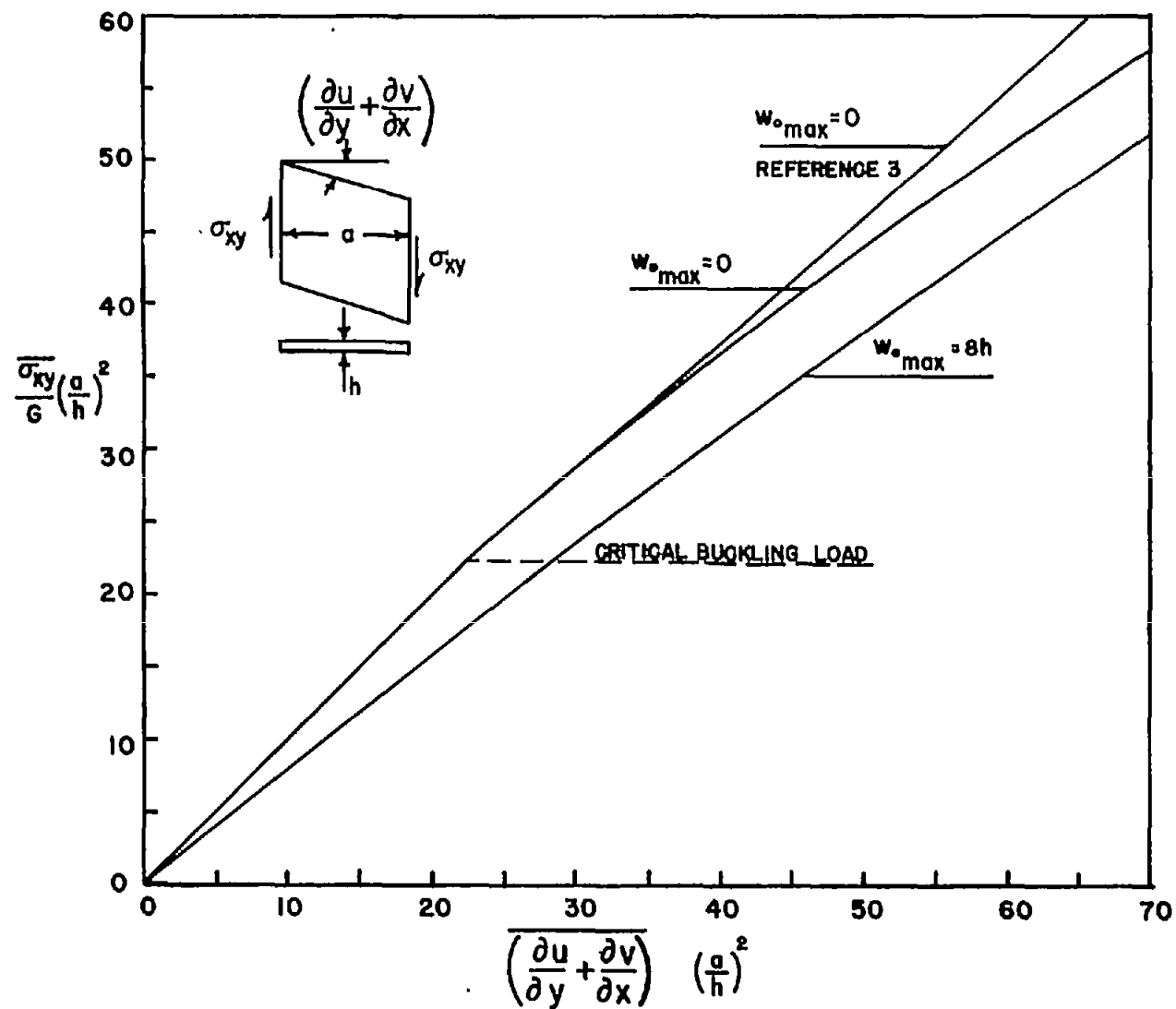Figure 4.- Large deflections of initially curved sheets under edge
compression.

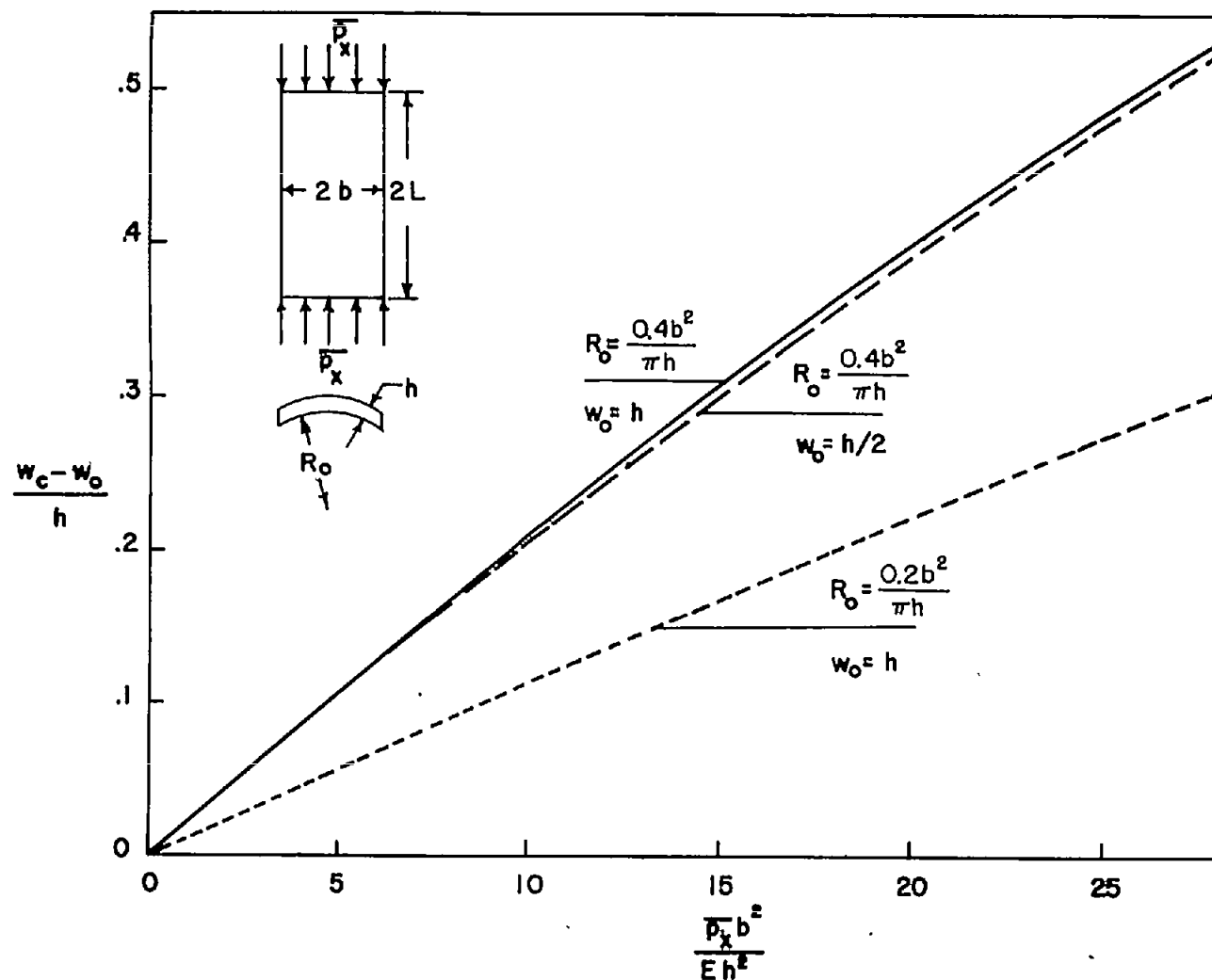Figure 5.- Shear loading versus average shear strain for initially curved
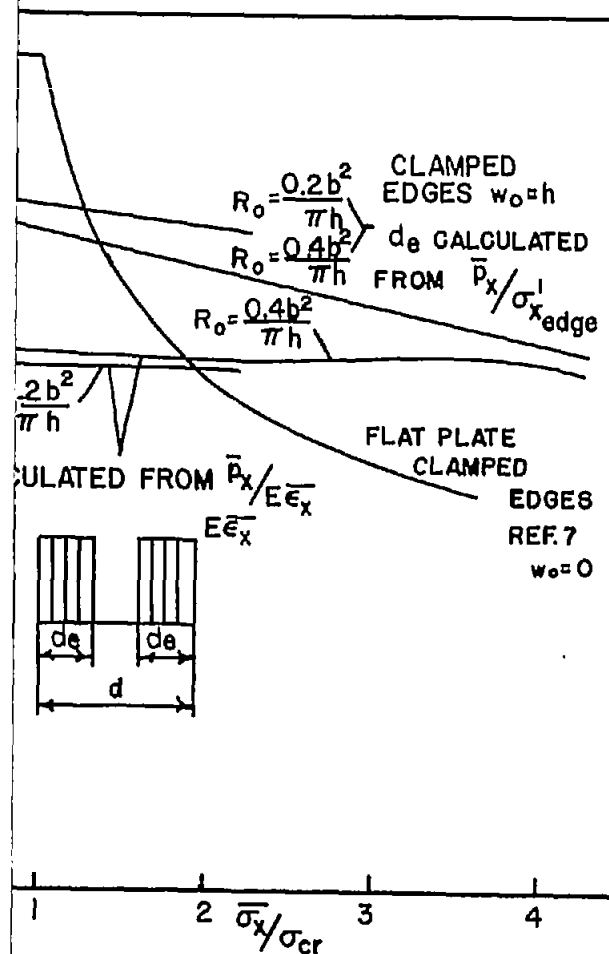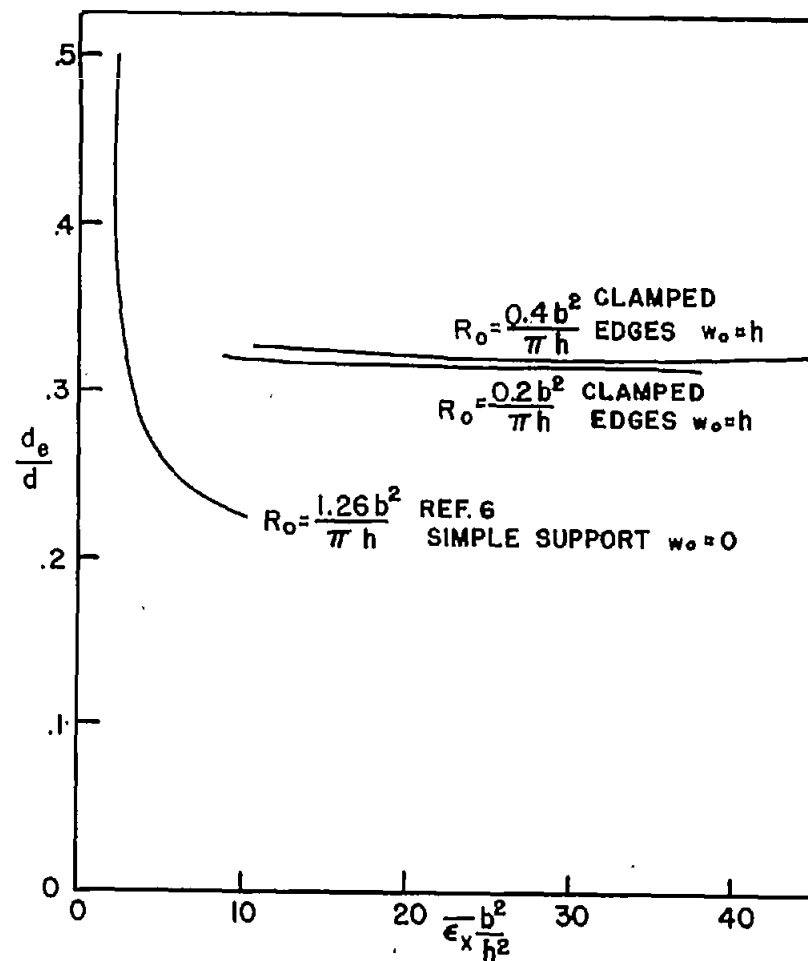square plate.

Figure 6.- Additional deflection for sheets with $1/R_0$ much greater than meridian curvature.

(a) Effective width ratio d_e/d against ratio average stress to critical stress.

(b) Effective width ratio d_e/d against edge-strain ratio.

Figure 7.- Effective width ratio d_e/d against stress and strain ratios.